Scanning Hall probe imaging of $ErNi_2B_2C$

Hendrik Bluhm, Suchitra E. Sebastian, Janice W. Guikema,* I. R. Fisher, and Kathryn A. Moler†
Departments of Physics and Applied Physics, Stanford University, Stanford, California 94305, USA
(Received 2 July 2005; revised manuscript received 7 November 2005; published 18 January 2006)

We report scanning Hall probe imaging of $ErNi_2B_2C$ in the superconducting, antiferromagnetic, and weakly ferromagnetic regimes in magnetic fields up to 20 Oe, well below H_{c1}, with two results. First, imaging isolated vortices shows that they spontaneously rearrange on cooling through the antiferromagnetic transition temperature T_N=6 K to pin on twin boundaries, forming a striped pattern. Second, a weak, random magnetic signal appears in the ferromagnetic phase below T_{WFM}=2.3 K, and no spontaneous vortex lattice is present down to 1.9 K. We conclude that ferromagnetism coexists with superconductivity either by forming small ferromagnetic domains or with oscillatory variation of the magnetization on sub-penetration-depth length scales.

DOI: 10.1103/PhysRevB.73.014514 PACS number(s): 74.25.Ha, 74.25.Qt, 75.60.−d, 75.50.Ee

I. INTRODUCTION

Magnetic order and superconductivity were once thought of as incompatible phenomena. The Meissner state excludes a magnetic field from the bulk, and superconductivity is destroyed by sufficiently high fields. However, two forms of coexistence are theoretically possible. First, if the orientation of local moments varies on a length scale shorter than the penetration depth, λ, the resulting internal field is not screened by the Meissner response, which is only effective over length scales of order of λ or larger.[1,2] This form of coexistence is found in $ErRh_4B_4$ and $HoMo_6S_8$.[3,4] The second possible form of coexistence is a so-called spontaneous vortex lattice which carries the field generated by the magnetization.[1,5,6] Such a spontaneous vortex lattice has never been observed in a zero-field-cooled sample, but $ErNi_2B_2C$ was suggested as a strong candidate.[5] Evidence for the existence of a vortex lattice in $ErNi_2B_2C$ after magnetic cycling has been reported[7] based on small-angle neutron scattering (SANS). The form of the coexistence in the zero-field-cooled state remains unclear.

In this work, we present local scanning Hall probe measurements of $ErNi_2B_2C$ at low fields with single-vortex resolution. Our results show clearly that no spontaneous vortex lattice forms after cooling in zero field. Instead, we observe a weak, random magnetic field, indicating that the magnetization is inhomogeneous on a submicron length scale. In addition, we show that vortices tend to locate along twin boundaries in the antiferromagnetic state. Earlier and recent work[8,9] using Bitter decoration demonstrated the tendency of vortices to locate along twin boundaries below T_N. With our technique we were able to examine the behavior of individual vortices in the three different phases of $ErNi_2B_2C$ and at the phase transitions.

$ErNi_2B_2C$ is a member of the quaternary rare earth compounds RNi_2B_2C (R represents rare earth), which show a variety of both magnetically ordered and superconducting states. Since their discovery one decade ago,[10–12] this family of materials has been under extensive study using a wide range of experimental techniques. $ErNi_2B_2C$ has a superconducting onset T_c of ≈11 K, becomes antiferromagnetic below $T_N \approx 6$ K,[13] and exhibits weak ferromagnetism below $T_{WFM} \approx 2.3$ K.[14] The magnetic phases at $T<6$ K are orthorhombic due to strong magnetostriction,[15] and the magnetism significantly enhances flux pinning.[16–18] Neutron scattering experiments[19,20] show that in $ErNi_2B_2C$, the antiferromagnetism in the temperature range $T_{WFM}<T<T_N$ occurs with an incommensurate wave vector of $0.553a^*$ (where $a^*=2\pi/a$) along the a axis with moments pointing in the $\pm b$ direction. At T_{WFM}, a lock-in transition to a commensurate wave vector of $0.55a^*$ takes place, suggesting that every 20th moment is left at a node of the staggered field and thus free to order ferromagnetically.[19,20] The resulting average ferromagnetic component of $0.39\mu_B$/Er is relatively weak and the self-field of $4\pi M=700$ G is comparable to the lower critical field $H_{c1}\approx 500$ Oe estimated from magnetization measurements in Fig. 1 and Ref. 13. The similarity of the self-field and H_{c1}, together with the persistence of superconductivity down to the lowest temperature explored so far, is the reason for suspecting a spontaneous vortex lattice.[5]

Possible scenarios for the interplay between superconductivity and ferromagnetism have been analyzed in Refs. 1, 2, 5, and 6 based on the Ginzburg-Landau free energies of a superconductor and a ferromagnet with magnetization $\vec{M}$ occupying the same space and coupled by a purely magnetic interaction term $1/4\pi\int\vec{B}\cdot\vec{M}$. Terms corresponding to pair breaking effects were considered less important since the magnetic moments are due to the partially filled $4f$ shells of the Er, which are not part of the conduction band. Reference 2 shows that supercurrents would screen out any magnetic field on length scales larger than the London penetration depth λ, so a phase transition leading to a homogeneous magnetization would be suppressed due to the screening of the magnetic coupling between the magnetic moments. Two different kinds of coexisting phases could emerge, depending on the coefficients of the model (particularly the magnetic coherence length ξ_M). First, if magnetic gradients are energetically cheap so that $\xi_M \ll \lambda$, $\vec{M}$ will oscillate with a wave vector of order $(\lambda\xi_M)^{-1/2}$. In an isotropic magnet this will always happen with a circular polarization so that $|\vec{M}|$ is constant and only gradient energy needs to be afforded. This spiral state has been reported in $ErRh_4B_4$ (Ref. 3) and $HoMo_6S_8$.[4] In the case of $ErNi_2B_2C$, however, a strong crystal electric field aligns the magnetic moments along the b axis,[19,20] so that the ordering is theoretically more likely to

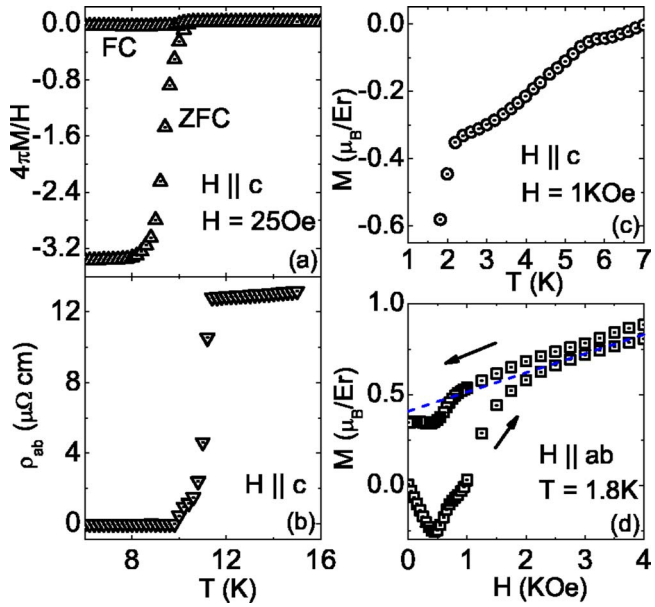

FIG. 1. (Color online) Sample characterization, (a) volume magnetization as a function of temperature in a magnetic field of 25 Oe applied parallel to the c axis. Both the zero-field-cooled (ZFC) and field-cooled (FC) data were taken on warming. (b) Zero field electrical resistivity in the ab plane ρ_{ab} as a function of temperature. (c) Temperature dependence of the magnetization in an applied field of 1 kOe applied parallel to the c axis, measured on warming following initial zero-field-cooling. (d) Magnetization as a function of applied field perpendicular to the c axis at $T=1.8$ K for increasing and decreasing field after zero-field cooling.

happen in a linearly polarized wave.[1] Second, if such a variation in $\vec{M}$ would be too costly and $4\pi M > H_{c1}$, a spontaneous vortex lattice may form, leading to a spatially varying $\vec{B}$ of uniform direction which can support a similar $\vec{M}$.[1,5] SANS experiments reported in Ref. 7 give evidence for such a vortex lattice in $ErNi_2B_2C$ after cycling to high fields. The vortex lattice peaks are absent after cooling in zero field, leaving open the question of the nature of the zero-field-cooled state.

II. SAMPLE PREPARATION AND METHODS

We have grown single crystals of $ErNi_2B_2C$ using a flux growth technique with Ni_2B as the flux.[13] Measurements were made on plates of typical size $3\times3\times0.5$ mm^3, where the crystallographic c axis is perpendicular to the plate surface. We measured magnetization and resistance using a Quantum Design SQUID magnetometer to confirm values of T_N, T_c, and T_{WFM} obtained in previous work.[13,14,19,20] The value of the superconducting transition temperature T_c is obtained from zero field resistivity and low-field ($H=25$ Oe) magnetization measurements. From Fig. 1, zero resistance and the sharp increase in diamagnetism which have previously been used to identify T_c (Ref. 13) appear at 10 K. The magnetization as a function of field at 1.8 K [Fig. 1(d)] indicates that $H_{c1,ab}$ is lower than 500 Oe. An extrapolation of the virgin curve magnetization data as indicated by the dashed line and the remnant magnetization give evidence for a ferromagnetically ordered moment of about $0.4\mu_B$/Er, consistent with Ref. 19. The temperature at which this weak ferromagnetic order sets in is inferred to be $T_{\mathrm{WFM}}=2.2$ K from the sharp break in the slope of magnetization as a function of temperature in an applied field of 1 kOe [Fig. 1(c)], indicating a phase transition at this temperature. The bump between 5 and 6 K in this figure can be attributed to the antiferromagnetic ordering at T_N, consistent with earlier work.[13,14,19,20]

To measure the local magnetic field component perpendicular to the sample surface, we used a scanning Hall probe microscope (SHPM) in a ^{4}He flow cryostat.[21] A 0.5 μm wide Hall probe defined using e-beam lithography on a 140 nm deep GaAs/AlGaAs heterostructure is scanned over the sample surface using a piezoelectric scanner. For some images requiring a good field resolution, we have averaged over several tens of scans and removed switching noise from the Hall probe from the raw data. The field sensitive area of the probe is located near a corner of the substrate so that an angle of a few degrees between the probe substrate and the sample lead to a probe-sample distance between 0.5 and 1 μm when the substrate corner touches the sample. Field components varying with a wave vector k in the xy plane are theoretically known to be attenuated as e^{-kz} at a height z above the sample.[22] The measured Hall voltage is proportional to the magnetic field averaged over the active area of the probe. Thus, both the probe's size and its height above the sample effect the spatial resolution.

This technique offers higher spatial resolution than magneto-optical measurements, is significantly faster and less dependent on surface quality than scanning tunneling spectroscopy, and allows many scans under different parameters in one cool-down. The information is easier to interpret than force gradients obtained from magnetic force microscopy (MFM).

Magnetic scans of the ab face were taken on a sufficiently large and smooth natural crystal face. Due to the crystal growth process, an area suitable for scanning was not available on a natural (010) plane. Thus we cut and polished the crystal along the ac (bc) face in order to scan there.

III. EXPERIMENTAL RESULTS

We first discuss the data taken on the ab face. Upon cooling the sample below T_c in a weak applied field, H_a, normal to the sample surface, vortices appear in a random configuration [Fig. 2(a)]. The vortex distribution is inhomogeneous, with a vortex density of H_a/Φ_0 (where $\Phi_0=h/2e$) within a factor of 2, as expected for a type II superconductor with pinning sites. Because of the large vortex spacing at $H_a \ll H_{c1}$, the repulsive interactions between the vortices are too weak to order the vortices into a lattice. Individual vortices occasionally move during scans. The apparent shape of the vortices, which depends mostly on the probe-sample separation, can be fitted well with a monopole model[23] for the vortex field in vacuum. The resulting flux per vortex is $(0.9\pm0.2)\ \Phi_0$ with the systematic uncertainty lying mostly in the spatial calibration of our microscope.

As the temperature is lowered below T_N, the vortices spontaneously line up along stripes with a typical separation

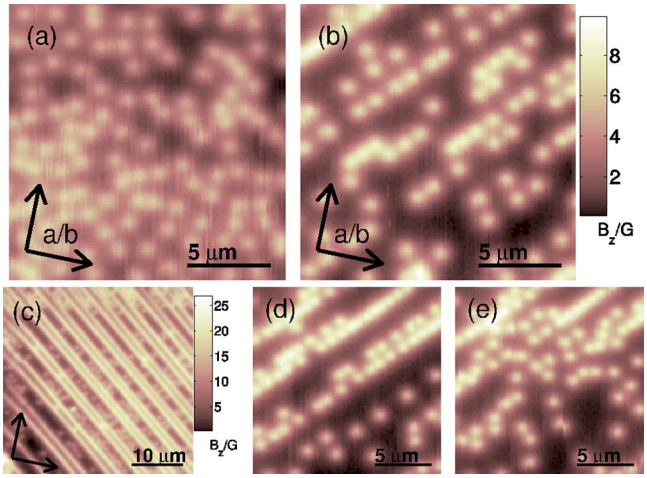

FIG. 2. (Color online) After cooling below T_c in a weak field [2.4 Oe in (a), (b), (d), (e), 18 Oe in (c)], a vortex distribution consistent with random pinning is observed on the *ab* face [(a) 7.3 K]. Upon reducing the temperature below T_N, the vortices spontaneously organize along twin domain walls along the [110] [(b) 5.3 K] or [$\bar{1}$10] [(c) 4.2 K] direction. The pattern gradually disappears as the temperature is raised again [(d) 5.7 K, (e) 6.0 K, different cycle than (a) and (b)]. The distance between the domain walls varies between typically 3 to 8 μm and their position and orientation changes after cycling above T_N. No further change is observed when cooling below T_{WFM}.

between stripes of 3 to 8 μm [Fig. 2(b)]. Between different cycles through T_N, their position varies and the orientation changes between the [110] or [$\bar{1}$10] [Fig. 2(c)] direction. As the largest stress due to the change in lattice parameters is likely to occur when only part of the sample has gone through the AFM transition, the exact configuration of the stripes can be expected to depend on such factors as temperature gradients and cooling rate during the transition. Further lowering the temperature below T_{WFM} has no effect on the vortices down to 1.9 K, the lowest temperature measured. As the temperature is raised above T_N, they move back into a nearly static disordered configuration [Figs. 2(d) and 2(e)]. This relaxation happens gradually over the course of several scans at 6 K. The remnants of the vortex alignment in Fig. 2(e) disappeared a few scans later without changing the temperature.

At temperatures above approximately 5 K, the vortices are still mobile enough to occasionally hop between different sites, both along and between twin boundaries, under the influence of the probe during scans. On the other hand, we observed no motion between two scans taken at 4 K, although the temperature was raised to 5.3 K for several hours in between. Thus, there is no evidence for thermally activated vortex motion. The depinning mechanism could be interaction with the field on the order of 0.5 Oe at the sample surface generated by the 10 μA rms ac bias of the Hall probe or mechanical or thermal effects due to local heating of the sample by the probe. Indeed, the depinning probability at a given T strongly depends on the probe-sample distance.

Below about 5 K, no vortex motion was observed. This is in good qualitative agreement with the depinning data in Refs. 16–18, where a gradual increase of the pinning strength with decreasing temperature above T_{WFM} and a relatively sharp increase upon cooling below T_{WFM} is reported.

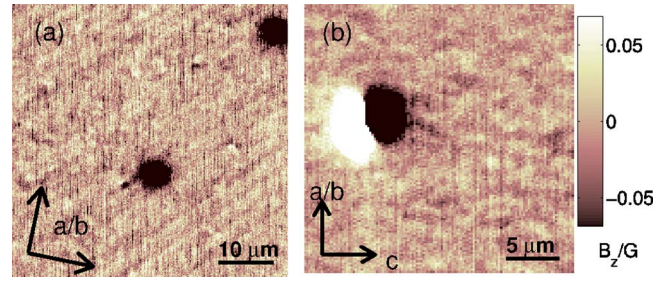

FIG. 3. (Color online) Magnetic images of the *ab* face (a) and *bc* face (b) at 1.9 K. Below T_{WFM} a weak random field of the order of 20 mG rms amplitude appears after (nominally) zero-field cooling. The blobs are vortices which saturate the color scale. If the random signal were due to the formation of an (unresolved) vortex lattice below T_{WFM}, one would expect any single vortex to be incorporated in the vortex lattice and disappear. The *ab* face (a) shows a structure at the same length scale and angle as the vortex lines revealing twin boundaries. Magnetic dipoles as in (b) have been observed only on the polished *bc* plane. We believe that they are vortex-antivortex pairs pinned on surface imperfections.

Our crystal growth process only yields natural faces at the (001) and what seems to be the (101)[(011)] plane, but with much smaller smooth patches in the latter case which makes imaging difficult. Scans along such a (101) face showed that vortices relocate there too as the temperature is changed, but we found no evidence for pinning in an ordered way, which is not surprising as the twin domains intersect the sample surface approximately at a 45° angle. Similar behavior was found on a cut and polished (100)[(010)] face, however obscured by vortex pinning at specific sites, which we attribute to crystal defects or surface damage probably due to the polishing process.

Upon cooling below T_{WFM}, a very weak magnetic signal with a seemingly random spatial variation of about 20 mG rms amplitude appears between the vortices, both on the *ab* and *ac*(*bc*) face (Fig. 3). However, we observe no change in the vortices on either surface at or below this transition. The scans on the *ab* plane show stripes in this signal which have the same typical width and angle as the twin domains revealed by vortices. No such striped structure is apparent on the *ac*(*bc*) face.

IV. DISCUSSION

In the following, we will first discuss the implication of our results for possible pinning mechanisms in the AFM and WFM regime and then proceed to the question of the ground state in the WFM phase.

The observed reorganization of the vortices along lines in the AFM phase was attributed in Refs. 8 and 9 to twin domain walls resulting from the strong magnetostriction in the magnetically ordered regime.[15] It was suggested there that the pinning is due to canting of the magnetic moments at the twin domain walls where the magnetically easy axis and thus

the orientation of the moments must change by 90°. Reference 8 also reports SHPM measurements at larger fields and without single vortex resolution. They observed an enhanced field near the domain walls, which they interpreted as "convincing evidence for local ferromagnetism at the domain walls."[8] Our data and also more recent Bitter decoration work[9] strongly suggest that this field variation is due to a higher vortex density at the twin boundaries.

The questions arise as to why vortices pin on domain walls, and to what extent canting moments at the domain walls are consistent with our results. We do not find any evidence for magnetic fields emerging from the twin boundaries beyond that of the vortices, so we can set a limit on the local magnetization strength at the twin boundaries. From the data in Fig. 3, we conclude that we would be able to detect a variation of B_z of 20 mG at the scan height z_0 above the sample. If the magnetization has a z-component $M_{z,0}$ over a width d along a domain wall and at least a few penetration depths into the sample, but vanishes away from the wall, the resulting far field at $z_0 \gg \lambda$, including the contribution of screening currents, is that of a quadrupole line and will have a maximum value of $8M_{z,0}d\lambda^2/(z_0+\lambda)^3$.[24] With $\lambda = 70$ nm (Ref. 25) and $z_0 = 0.7\ \mu$m, we conclude that $M_{z,0}d < 0.3\text{G}\mu\text{m}^2$. For a plausible d of 10 nm, this gives upper limits $M_{z,0} < 30$ emu/cm^3 and $B_z = 4\pi M_{z,0} < 400$ G at the domain wall. The linear flux density of 4 Gμm of such a domain wall would correspond to only one vortex every 5 μm, which is much less than the vortex accumulation seen in Fig. 2(c), for example. This upper limit to the flux density suggests that some pair breaking mechanism rather than a purely magnetic interaction plays an important role in pinning the vortices at twin boundaries.

Similar considerations apply to the much stronger pinning mechanism below T_{WFM}.[16,18] Strong gradients in $\vec{M}$ could lead to enhanced pair breaking and a reduced condensation energy at domain walls. Alternatively, shielding currents at the domain walls might pull vortices into domains with $\vec{M}$ aligned with the vortex field. However, the latter effect is likely to be weak if $\vec{M}$ varies on a sub-penetration-depth length scale and one would expect a clearly reduced pinning strength for vortices along the c axis as they would be orthogonal to $\vec{M}$, contrary to observation.[16]

We now turn to the implications of our results regarding the existence of a spontaneous vortex phase. The fact that no vortex relocation is observed when cooling through T_{WFM} clearly indicates that no vortex lattice or other vortex state is formed. If the random signal seen at 1.9 K were due to the formation of vortices, which might in principle happen in a disordered manner without a net magnetization, the previously isolated vortices would interact with the newly formed ones and should be annihilated or screened. Thus we conclude that the magnetization must vanish when averaged over several μm, but has local variations that are not fully screened and appear in our data.

To extract information about the magnetization $\vec{M}$ in the sample from this random signal, the following must be considered: Due to the separation between the sensor and the sample surface, z_0, components in the spectrum of the image with a large wave number k will be attenuated exponentially by a factor e^{-kz_0}.[22] In addition, averaging occurs due to the finite probe size. This effective absence of large k information makes a deconvolution of the data to obtain the magnetic field at the sample surface impossible. On the other hand, any slow variation of $\vec{M}$ with $k \lesssim 1/\lambda$ will be screened by shielding currents.[24] As $\lambda \approx 70\ \text{nm} \ll z_0$,[25] only the strongly attenuated small wave vector region of the spectrum of $\vec{M}$ is manifest in our data. This means that there is a wide range of possible scenarios for the behavior of $\vec{M}$ which would be consistent with our data. Yet, there must be some degree of randomness, because the correlation length of the ferromagnetic oscillation must be less than a few μm to explain the random signal we see. We conclude that after cooling in zero field, the ferromagnetism has either a domainlike or an oscillatory structure similar to that found in $ErRh_4B_4$ and $HoMo_6S_8$, where a relatively broad peak in the neutron spectrum is observed[3,4] at long wavelengths. Neutron scattering[19,20] and high field susceptometry[14] data on $ErNi_2B_2C$ show that well below T_N, the spins are fixed in direction (up to twinning) and can only change sign. Therefore, this ferromagnetic structure is likely to be squared up, just as the antiferromagnetic spin density wave. If the local magnetization strength is on the order of the bulk remnant magnetization observed after field cycling, the domains must be much smaller than 1 μm to explain the low signal level. A model with the magnetic domains coinciding with the several μm large twin domains (regardless of the strong shielding over such length scales) would lead to an about 3 orders of magnitude larger signal at the domain walls[24] and thus can be ruled out.

For a more quantitative analysis, we estimated the spectral densities $S_{B_z} = \int d^2\vec{r}\langle B_z(\vec{r})B_z(\vec{r}+\vec{r}')\rangle e^{-i\vec{q}\cdot\vec{r}'}$ of the magnetic scans in Fig. 3 by averaging the modulus square of the FFT of segments of the image. The segments were chosen half as big as the image and multiplied with a windowing function. To obtain the spectrum of Fig. 3(a), fits of the vortices were subtracted so that the whole image could be used. For Fig. 3(b), fitting attempts lead to large residuals so that we used only segments not strongly affected by the vortex field. The results are shown in Fig. 4. To come up with a theoretical model, we assume that the magnetization pattern can be described by a spectral density $S_{M,\alpha\beta}(\vec{q}) = \int d^3\vec{r}'\langle M_\alpha(\vec{r})M_\beta(\vec{r}+\vec{r}')\rangle e^{-i\vec{q}\cdot\vec{r}'}$ with $\alpha,\beta = x,y,z$. According to the arguments of Sec. I, it is reasonable to furthermore assume that the characteristic length scales of the variation of $\vec{M}$ are much shorter than λ and z_0, so that $S_{M,\alpha\beta}(\vec{k})$ will not have a strong $\vec{k}$ dependence for $k \lesssim 1/\lambda$. One can show that under those assumptions and with a predominantly in-plane orientation of $\vec{M}$, say along the x direction, $S_{B_z}(\vec{k}) = 8\pi^2\lambda k_x^2 e^{-2k(z_0+\lambda)} S_{M,xx}(0)$.[24]

A comparison of this model [Fig. 4(c)] and the spectral density [Fig. 4(b)] of the $ac(bc)$-face scan from Fig. 3(b) demonstrates a good qualitative agreement. The large fluctuations in the experimental spectrum due to lack of better statistics forbid a more quantitative comparison. By comparing the magnitude of the data and the model, we obtain $S_{M,xx}(0) \approx 5\times 10^{-4}\ \text{G}^2\mu\text{m}^3$. If the variation in the domain size is on the order of their typical size so that the correlator

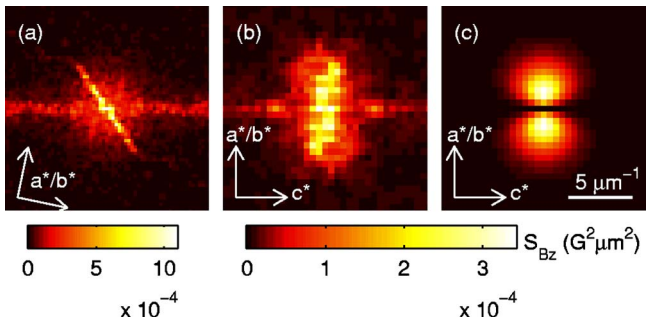

FIG. 4. (Color online) Panels (a) and (b) show estimates of the spectral densities of Figs. 3(a) and 3(b). The faint horizontal lines at $k_y=0$ and the sharp peak at the origin are scanning artifacts due to sensor noise. Panel (c) shows the spectrum $S_{B_z}(\vec{k})$ expected for a magnetization in the a/b direction with all characteristic length scales of M shorter than $\min(\lambda, z_0)$. This model shows reasonable agreement with the data in (b). All plots are shown on the same scale with $k=0$ in the center.

$\langle M_x(\vec{r})M_x(\vec{r}+\vec{r}')\rangle$ is mostly positive, $S_{M,xx}(0)$ can be interpreted as the product of a coherence volume with the typical magnetization strength $\langle M_x^2\rangle$. Using $4\pi\sqrt{\langle M_x^2\rangle}=700$ G, one obtains an estimate of 400 nm^3 or 3000 unit cells for the domain volume. However, one should keep in mind that this interpretation is meaningless for an oscillatory magnetization.

The spectral density obtained from the *ab*-face scan [Fig. 3(a)] as shown in Fig. 4(a) on the contrary is dominated by the diagonal feature near $\vec{k}=0$, which stems from the stripes in the scan. Its narrow shape indicates a long correlation length on the order of the scan size or larger parallel to the stripes. This suggests that there is a net average magnetization related to the twin boundaries which does not change signs over at least tens of μm. It is interesting to note that this observation implies that there is a preferred field direction attached to either the twin domains or their boundaries. Additionally, Fig. 4(a) shows a broader, isotropic peak. This is probably of similar origin as the peaks in Fig. 4(b). The lack of anisotropy can be explained by averaging over different orientations of the easy axis in different twin domains.

Our main result is thus that in near zero field, no magnetization-induced vortices appear down to 1.9 K. In other words, $ErNi_2B_2C$ shows no spontaneous vortex lattice in the strictest sense, which would form upon cooling below the ferromagnetic transition temperature in zero field. However, the term "spontaneous" has also been used to describe a vortex lattice that forms only when aligning the magnetic domains with a sufficiently large magnetic field, but persists after returning to zero field. SANS experiments[7] on $ErNi_2B_2C$ indeed detect a lattice after, but not before cycling the field. However, the absence of the SANS vortex lattice signal in a zero-field-cooled process does not imply the absence of vortices. Their configuration could be too disordered, or the vortex density could be too low because of hysteresis for a distinct signal to appear in the neutron data. In contrast, our results clearly indicate that there are no magnetization-induced vortices in the zero-field-cooled WFM state.

Combining our results with the SANS observation of a vortex lattice after cycling in a field, it appears that there are two metastable states at zero field in the superconducting ferromagnetic regime. It remains unclear which one of these is the true ground state. The strong vortex pinning could prevent a relaxation of the vortex state into the vortex free state after cycling the field, even if the latter would have a lower energy. In the spatially resolved magnetization data of Ref. 18, a maximum of some 850 G in the magnetic field was found in the middle of the sample when reducing the applied field from higher values to about 700 Oe, giving evidence for strong bulk pinning, rather than edge barrier effects. The pinning-induced field gradients reported there are on the order of 3 G/μm. This suggests that vortex pinning might be sufficient to maintain the magnetization after field cycling and possibly cause a vortex lattice to persist. If so, one would expect the field cycled zero field average magnetization to depend strongly on the sample size. Comparing the data from Refs. 16 and 19 and Fig. 1(d) indeed show variations by about a factor of 2, but not as large as one might expect from the differences in sample size. However, pinning alone cannot explain the observed anisotropy of the remnant magnetization because the flux pinning appears to be relatively isotropic.[7] This suggests that the *ab*-plane ferromagnetism does play a role in stabilizing the vortex lattice by reducing the vortex repulsion or the attraction of vortices to the sample edges and thus lowering the vortex energy. In a simple picture, once the ferromagnetic domains are aligned it would be unfavorable for a single vortex to leave the crystal below a certain vortex density even with no applied field because the internal magnetization acts as an applied field. This explanation would come very close to the notion of a spontaneous vortex lattice. It should be possible to test this hypothesis by observing the behavior of the magnetic induction (likely carried by vortices) near the edges of the sample near zero applied field after field cycling. If only bulk pinning is relevant, the field (and hence vortex density) should tend to zero approximately linearly towards the edge of the sample over macroscopic distances. If, on the other hand, the vortices are stabilized by an internal magnetization, one would expect a significant flux density penetrating the samples near the edges. Such an experiment could be carried out using scanning Hall probes, but magneto-optical imaging may also be suitable.

If the energy of the field-cycled zero-field vortex state is indeed lower than that of the zero-field-cooled state observed in this work, one may ask why the transition between the two states upon reducing the temperature at zero field seems inhibited, that is why there is no accessible transition pathway. As the superconductivity is already fully developed at T_{WFM}, the only way for vortices to form would be to enter through the sample edge. Just as in ordinary superconductors, this requires an edge barrier to be overcome, which however may be modified in a nontrivial way by the ferromagnetism. Furthermore, it is not *a priori* clear if the energy of an isolated vortex with the moments aligned only in the region with a substantial field near its core is lower than that of the Meissner state, even if this would be the case for a fully developed spontaneous vortex lattice. Indeed, an attractive long range vortex interaction was predicted under certain assumptions in Ref. 6 in the presence of ferromagnetism.

Another interesting consideration is that with a fully developed internal field, the magnetic energy is $2\times 700\ \mathrm{G} \times 7.8\mu_B/k_B = 0.7\ \mathrm{K}/k_B$ per Er atom. Thus, the Meissner screening might suppress the ferromagnetic transition by roughly the same amount from the value of 2.2 K obtained from magnetization measurements well above H_{c1}. This might explain the hysteresis in the ferromagnetic transition mentioned by Kawano *et al.*[19] and suggests that experiments extending to lower temperatures might reveal interesting effects. A hint of those has been given in Ref. 26 where a peak in a 21 MHz $\Delta\lambda$ measurement appears at 0.45 K. This effect has been interpreted as thermally activated switching of a vortex lattice, but given the indirectness of the measurements, it is not clear that this is the only possible interpretation. Furthermore, measurements with smaller probes and a reduced sample-to-probe separation may provide more quantitative data about the domain structure and would allow single vortex resolution at higher applied fields. The observation of interacting vortices along the twin domain walls and attempts to systematically manipulate them might reveal information about the pinning potential.

In conclusion, we have observed the pinning of vortices and the development of ferromagnetism in $ErNi_2B_2C$ in small applied fields. In the antiferromagnetic phase, vortices are weakly pinned on twin domain boundaries due to the magnetostriction-induced orthorhombic to tetragonal transition associated with the antiferromagnetic order. In the ferromagnetic regime, no spontaneous vortex lattice is seen, and a very weak random magnetic signal develops, indicating the formation of domains or oscillatory order which might explain the strong increase in pinning.

ACKNOWLEDGMENTS

The authors would like to thank Paul Canfield for useful discussions and providing Ref. 9 before publication. This work was supported by the Department of Energy under Contract No. DE-AC02-76SF00515. Two of the authors (I.R.F.) and (S.S.) were supported by the National Science Foundation, Division of Materials Research under Grant No. DMR-0134613.

*Present address: Department of Physics, Cornell University, Ithaca, NY 14853.

†Electronic address: kmoler@stanford.edu

[1] H. S. Greenside, E. I. Blount, and C. M. Varma, Phys. Rev. Lett. **46**, 49 (1981).

[2] E. I. Blount and C. M. Varma, Phys. Rev. Lett. **42**, 1079 (1979).

[3] D. E. Moncton, D. B. McWhan, P. H. Schmidt, G. Shirane, W. Thomlinson, M. B. Maple, H. B. MacKay, L. D. Woolf, Z. Fisk, and D. C. Johnston, Phys. Rev. Lett. **45**, 2060 (1980).

[4] J. W. Lynn, G. Shirane, W. Thomlinson, and R. N. Shelton, Phys. Rev. Lett. **46**, 368 (1981).

[5] T. K. Ng and C. M. Varma, Phys. Rev. Lett. **78**, 330 (1997).

[6] C. G. Kuper, M. Revzen, and A. Ron, Phys. Rev. Lett. **44**, 1545 (1980).

[7] H. Kawano-Furukawa, E. Habuta, T. Nagata, M. Nagao, H. Yoshizawa, N. Furukawa, and H. T. K. Kadowaki, cond-mat/0106273 (unpublished).

[8] N. Saha, R. Surdeanu, M. Marchevsky, G. J. Nieuwenhuys, C. D. Dewhurst, R. J. Wijngaarden, D. M. Paul, and P. H. Kes, Phys. Rev. B **63**, 020502(R) (2000).

[9] L. Y. Vinnikov, J. Anderegg, S. L. Bud'ko, P. C. Canfield, and V. G. Kogan, Phys. Rev. B **71**, 224513 (2005).

[10] T. Siegrist, H. W. Zandbergen, R. J. Cava, J. J. Krajewski, and W. F. Peck, Nature (London) **367**, 254 (1994).

[11] H. Eisaki, H. Takagi, R. J. Cava, B. Batlogg, J. J. Krajewski, W. F. Peck, K. Mizuhashi, J. O. Lee, and S. Uchida, Phys. Rev. B **50**, R647 (1994).

[12] R. J. Cava, H. Takagi, H. W. Zandbergen, J. J. Krajewski, W. F. Peck, T. Siegrist, B. Batlogg, R. B. Vandover, R. J. Felder, K. Mizuhashi, J. O. Lee, H. Eisaki, and S. Uchida, Nature (London) **367**, 252 (1994).

[13] B. K. Cho, P. C. Canfield, L. L. Miller, D. C. Johnston, W. P. Beyermann, and A. Yatskar, Phys. Rev. B **52**, 3684 (1995).

[14] P. C. Canfield, S. L. Budko, and B. K. Cho, Physica C **262**, 249 (1996).

[15] C. Detlefs, A. H. M. Z. Islam, T. Gu, A. I. Goldman, C. Stassis, P. C. Canfield, J. P. Hill, and T. Vogt, Phys. Rev. B **56**, 7843 (1997).

[16] P. L. Gammel, B. Barber, D. Lopez, A. P. Ramirez, D. J. Bishop, S. L. Bud'ko, and P. C. Canfield, Phys. Rev. Lett. **84**, 2497 (2000).

[17] C. D. Dewhurst, S. S. James, R. A. Doyle, Y. Paltiel, H. Shtrikman, E. Zeldov, and D. McK. Paul, Phys. Rev. B **63**, 060501(R) (2000).

[18] S. S. James, C. D. Dewhurst, S. B. Field, D. McK. Paul, Y. Paltiel, H. Shtrikman, E. Zeldov, and A. M. Campbell, Phys. Rev. B **64**, 092512 (2001).

[19] H. Kawano-Furukawa, H. Takeshita, M. Ochiai, T. Nagata, H. Yoshizawa, N. Furukawa, H. Takeya, and K. Kadowaki, Phys. Rev. B **65**, 180508(R) (2002).

[20] S. M. Choi, J. W. Lynn, D. Lopez, P. L. Gammel, P. C. Canfield, and S. L. Bud'ko, Phys. Rev. Lett. **87**, 107001 (2001).

[21] J. W. Guikema, Ph.D. thesis, Stanford University, 2004.

[22] B. J. Roth, N. G. Sepulveda, and J. P. Wikswo, J. Appl. Phys. **65**, 361 (1989).

[23] J. Pearl, J. Appl. Phys. **37**, 4139 (1966).

[24] H. Bluhm (unpublished).

[25] P. L. Gammel, B. P. Barber, A. P. Ramirez, C. M. Varma, D. J. Bishop, P. C. Canfield, V. G. Kogan, M. R. Eskildsen, N. H. Andersen, K. Mortensen, and K. Harada, Phys. Rev. Lett. **82**, 1756 (1999).

[26] E. E. M. Chia, M. B. Salamon, T. Park, H.-J. Kim, and S.-I. Lee, cond-mat/0409521 (unpublished).